Applied Catalysis B: Environmental 86 (2009) 190–195

Contents lists available at ScienceDirect

Applied Catalysis B: Environmental

journal homepage: www.elsevier.com/locate/apcatb

Promotional effect of H_2 on CO oxidation over Au/TiO_2 studied by operando infrared spectroscopy

Laurent Piccolo [a,*], Helen Daly [b], Ana Valcarcel [a], Frédéric C. Meunier [b,c]

[a] Université Lyon 1, CNRS, UMR 5256, IRCELYON, Institut de Recherches sur la Catalyse et l'Environnement de Lyon, 2 Avenue Albert Einstein, F-69626 Villeurbanne, France
[b] CenTACat, Queen's University Belfast, David Keir Building, Stranmillis Road, BT9 5AG Belfast, Northern Ireland, United Kingdom
[c] Laboratoire Catalyse et Spectrochimie, ENSICAEN-Université de Caen-CNRS, 6 Boulevard du Maréchal Juin, F-14050 Caen Cedex, France

ARTICLE INFO

Article history:
Received 16 June 2008
Received in revised form 31 July 2008
Accepted 1 August 2008
Available online 22 August 2008

Keywords:
CO oxidation
PrOx
Gold catalysis
DRIFTS
Operando spectroscopy

ABSTRACT

The oxidation of carbon monoxide in the presence of various concentrations of molecular hydrogen has been studied over a Au/TiO_2 reference catalyst by combining diffuse reflectance infrared Fourier transform spectroscopy (DRIFTS) and mass spectrometry. It is shown for the first time that H_2 enhances the CO oxidation rate on Au/TiO_2 without leading to any major loss of selectivity. Increasing the H_2 pressure induces higher CO and H_2 oxidation rates. Under H_2-free conditions, the surface species detected are $Au^{\delta+}$–CO, Ti^{4+}–CO, carbon dioxide and carbonates. Upon the addition of H_2, Au^0–CO, water and hydroxyl groups become the main surface species. The occurrence of a preferential CO oxidation mechanism involving H_xO_y species under the present experimental conditions is proposed.

1. Introduction

Carbon monoxide oxidation over gold catalysts is a promising system for low-temperature applications such as air decontamination and fuel cells (since preferential oxidation of CO [PrOx] can be used to purify hydrogen fuel [1]). From a fundamental point of view, in spite of the "gold rush" which began 20 years ago [2], the mechanism of gold-catalyzed CO oxidation is still under debate [3–6].

Since the work of Haruta and co-workers [7], there have been many reports on oxide-supported gold catalysts working in PrOx conditions, typically ~80 °C with large hydrogen excess (~70 mol.%) (see, e.g., Refs. [8–12]), but few attempts to analyze *the effect of H_2 addition* on the CO oxidation mechanism [13–15]. Conversely, numerous studies have focused on the effect of H_2O addition [8,9,12,13,16–22], which is present under PrOx conditions. In particular, Daté et al. have shown that water promotes CO oxidation on Au/TiO_2, Au/Al_2O_3 and Au/SiO_2, and have proposed a mechanism in which H_2O allows O_2 activation and decomposition of carbonate by-products [19].

It has been demonstrated that hydrogen has a similar promotional effect. Depending on the experimental conditions, it can prevent deactivation, regenerate the catalyst or even accelerate CO_2 formation, especially for catalysts usually poorly active in pure CO oxidation, such as Au/Al_2O_3 [10–13,15,21,23,24]. In the presence of H_2, Au/Al_2O_3 has been found as active as Au/TiO_2 [11], which is one of the best systems for pure CO oxidation. By investigating the effect of both molecules, it has been proposed that the positive influence of H_2 and H_2O on the activity of Au/Al_2O_3 may be of a similar nature [5,12]. Recently, Quinet et al. have investigated the kinetics of PrOx on Au/Al_2O_3 [24]. These authors have shown that hydrogen enhances the CO oxidation rate even at low concentrations, possibly by reacting with oxygen to form hydroperoxy intermediates that selectively react with CO. A similar mechanism has been proposed to explain the promoting effect of H_2 on unsupported gold, which thus appears to be intrinsically active [23].

In a comprehensive diffuse reflectance infrared Fourier transform spectroscopy (DRIFTS) study of PrOx on Au/TiO_2 in large H_2 excess, Schumacher et al. have observed that the presence of H_2 inhibits the formation of carbonate-like species that develop in $CO + O_2$ mixtures [10]. The formation of these species, which have also been directly identified by others on the same catalyst [5,16,25–29], favors deactivation [5,9,10,19,26]. We have further shown that, similarly to water, *low pressures* of H_2 are sufficient to regenerate Au/TiO_2 [15]. However, an investigation of the PrOx mechanism using simultaneous infrared and kinetic analyses is

* Corresponding author.
E-mail address: laurent.piccolo@ircelyon.univ-lyon1.fr (L. Piccolo).

0926-3373/$ – see front matter © 2008 Elsevier B.V. All rights reserved.
doi:10.1016/j.apcatb.2008.08.011

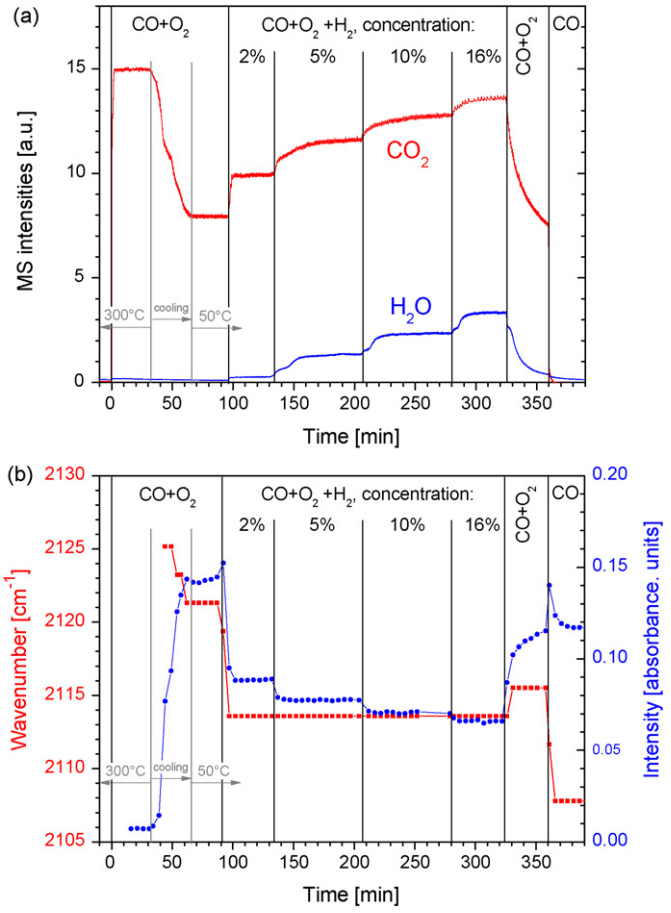

Fig. 1. (a) Mass spectrometry signals for CO_2 (m/z = 44, red, top curve) and H_2O (m/z = 18, blue, bottom curve). Experimental conditions are reported on the graph, except CO and O_2 molar fractions: 2 mol.%. (b) Position (red squares/left scale) and intensity (blue disks/right scale) of the main Au-carbonyl peak (see Fig. 4) under the same conditions as in (a). (For interpretation of the references to color in this figure legend, the reader is referred to the web version of the article.)

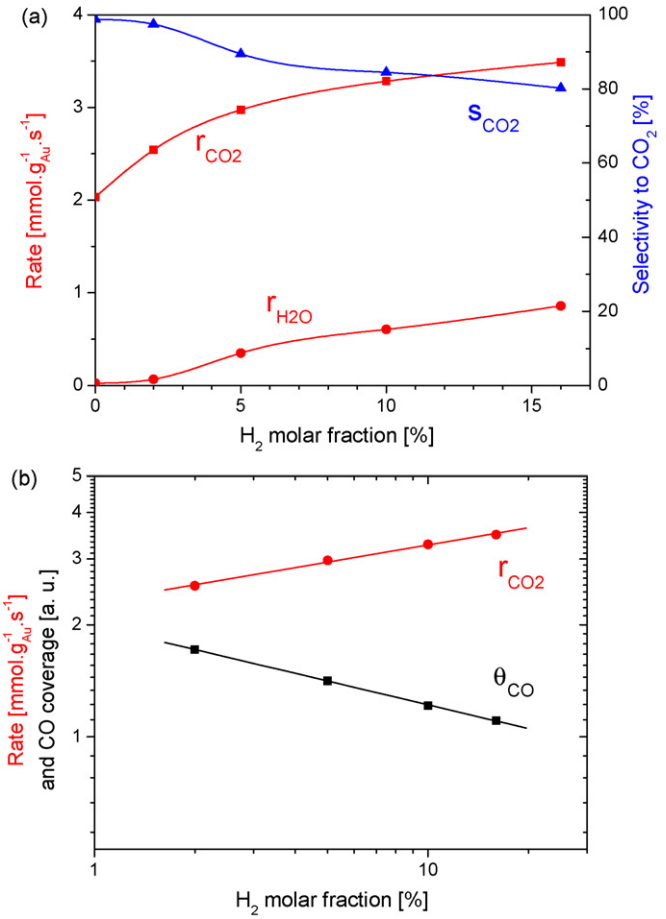

Fig. 2. (a) Rates of CO_2 (red squares) and H_2O (red circles) formations (left scale), and selectivity to CO_2 (blue/right scale) versus H_2 content in the 2% CO + 2% O_2 + He feed at 50 °C. Y scales allow CO conversion to be directly obtained from the r_{CO2} trace, using the right Y-axis. Quasi steady-state conversion values (measured at the end of each pressure stage) have been used for the rate calculations. (b) Rate of CO_2 formation (red circles) and CO coverage (black squares) versus H_2 content (log–log plot). The coverage of CO on Au (θ_{CO}, in absorbance cm^{-1} units) is the area of the ν(C–O) band (see Fig. 4), including gas-phase CO correction. The slope of r_{CO_2} and θ_{CO} linear fits are 0.153 ± 0.007 and −0.212 ± 0.002, respectively. (For interpretation of the references to color in this figure legend, the reader is referred to the web version of the article.)

still lacking. In this article, we report on the first combined in situ/transient kinetic study of PrOx over Au/TiO_2.

2. Experimental

The experimental setup consisted of a high-temperature DRIFTS cell (from Spectra-Tech) fitted with ZnSe windows. The cell was located in a FTIR spectrometer (Bruker Equinox 55) operating at a resolution of 4 cm^{-1}. The reactor crucible was modified to ensure plug-flow conditions throughout the catalyst bed: the original porous bed supporting the sample was replaced by an inert metallic mesh and Teflon tape was used to seal the gap between the ceramic crucible and the metallic base plate [30]. The reaction flow was going down through the reactor bed, so that the upper layer of the catalyst (which is probed by DRIFTS) was the front of the bed. The cell was connected to the feed gas cylinders through low-volume stainless-steel lines. A cold trap containing solid CO_2 and acetone was used to avoid possible contamination of the catalyst by the feed gases. The gas flows were adjusted by mass flow controllers (from Aera). The cell outlet was connected to a quadrupole mass spectrometer (Hiden Analytical HPR20) via a warm capillary.

The Au/TiO_2 reference catalyst (Type A, lot. No. Au–TiO_2 #02-07, sample No. 105) was manufactured by Süd-Chemie Catalysts (Japan) under the supervision of Haruta, characterized by Tsubota and co-workers and provided by the World Gold Council (WGC). The sample preparation followed a deposition–precipitation protocol developed by Haruta and co-workers [25]. The gold loading and particle size were 1.5 ± 0.1 wt.% and 3.3 ± 0.7 nm, respectively, as indicated by the WGC.[1] The amount of catalyst used in the DRIFTS reactor was 25 ± 5 mg.

The catalyst was pretreated in the DRIFTS–MS setup by heating to 300 °C (heating rate 10 °C min^{-1}) in He flow, then by exposure to CO (2 mol.%) + O_2 (2 mol.%) + He (total flow rate 100 mL min^{-1} at atmospheric pressure) at 300 °C. Afterwards the sample was cooled down to 50 °C (cooling rate 20 °C min^{-1}), temperature at which the experiment was then carried out. Masse/charge ratios 18, 28, 32 and 44, corresponding to H_2O, CO, O_2 and CO_2, respectively, were continuously monitored by mass spectrometry (MS). No corrections due to spectrometer sensitivity were made to the MS data. Increasing H_2 molar fractions (2, 5, 10 and 16 mol.%) were added to the CO (2 mol.%) + O_2 (2 mol.%) + He flow.

The DRIFTS data are reported as log $1/R$ ("pseudo absorbance"), with $R = I/I_0$, where R is the sample reflectance, I the intensity

[1] Na concentration: 0.037 wt.%.

measured under reaction conditions, and I_0 the intensity measured on the sample under helium flow (see Refs. [31,32] for more details). In this work, the I_0 background spectrum was recorded at 300 °C, just before introduction of the reactant mixture.

3. Results and discussion

Fig. 1a shows the CO_2 and H_2O MS signals during the full CO oxidation/PrOx experiment. DRIFTS spectra were recorded at each stage of this experiment. Fig. 1b plots the position and intensity of the carbonyl DRIFTS band (see below) versus time. Fig. 2 depicts the evolution of the reaction rates, selectivity (CO_2 formation rate divided by CO consumption rate) and CO coverage as a function of the H_2 molar fraction. CO conversions can also be determined from Fig. 2a (see caption). Fig. 3 shows complete DRIFTS spectra recorded at 50 °C in the absence and in the presence of H_2, along with the main vibration modes and assignments. Figs. 4–6 show the carbonyl, carbonate-like and hydroxyl/water regions of the DRIFTS spectra, respectively (recording times are indicated on the right side of each figure, using the same timescale as in Fig. 1).

3.1. Gas-phase products

At 300 °C, the CO conversion reaches ~95% (as deduced from the CO MS signal [not shown] and taking into account the fragmentation pattern of ca. 9 and 1 for the CO_2 signal at $m/z = 44$ and 28, respectively). During sample cooling to 50 °C, the conversion decreases to ~50%. The 50% conversion point corresponds to a rate of 2.0 $mmol_{CO}\ g_{Au}^{-1}\ s^{-1}$, i.e., 0.43 $mol_{CO}\ mol_{Au}^{-1}\ s^{-1}$, that is a TOF per Au surface atom equal to 1.3 s^{-1}, which is in accordance with the published data for highly active catalysts [5].

Introduction of 2% H_2 induces a fast increase of the CO_2 signal and the formation of a very small amount of water, giving rise to a high selectivity to CO_2 with respect to H_2O (>98%), as shown in Fig. 2a. Higher H_2 molar fractions (5, 10 and 16 mol.%) lead to higher CO_2 and H_2O formation rates. With 16% H_2, CO_2 formation rate is about twice its value without H_2. The selectivity to CO_2 decreases as H_2 percentage increases, but remains above 80% for 16% H_2 (Fig. 2a).

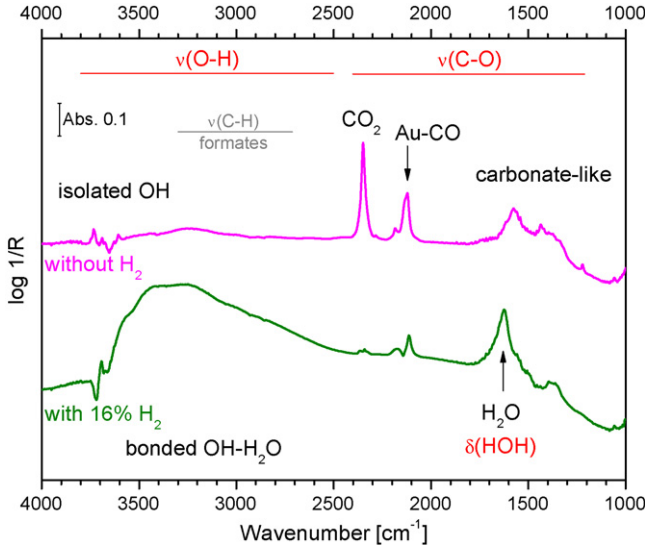

Fig. 3. Overview of the features detected by DRIFTS for Au/TiO_2 exposed to 2% CO + 2% O_2 in He (top spectrum, recorded at $t = 87$ min, see Fig. 1) and 2% CO + 2% O_2 + 16% H_2 in He (bottom spectrum, recorded at $t = 322$ min) at 50 °C. Corresponding vibration modes and surface species are indicated. Abs. means "pseudo absorbance" in log $1/R$ units (see Section 2).

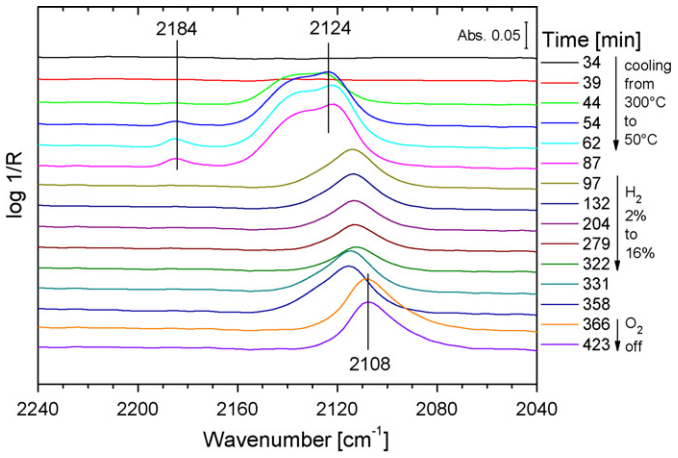

Fig. 4. Carbonyl region (C–O stretching mode) of DRIFTS spectra recorded at various times of the experiment depicted in Fig. 1. The gas-phase CO contribution was subtracted from the spectra.

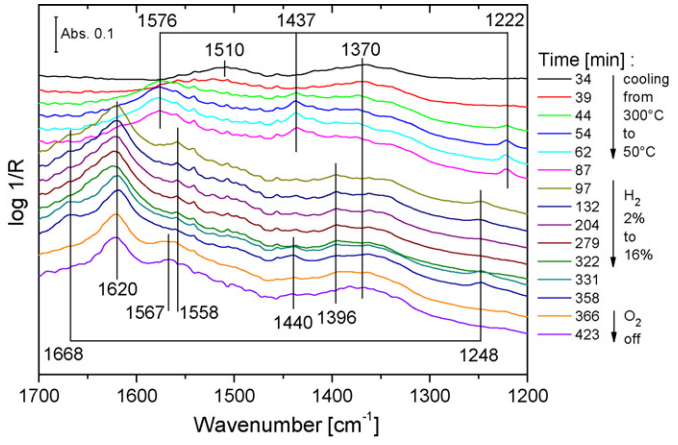

Fig. 5. Carbonate (mainly C–O stretching mode) and adsorbed water (H–O–H bending mode) region of DRIFTS spectra (same spectra as in Fig. 4). Horizontal lines link associated peaks.

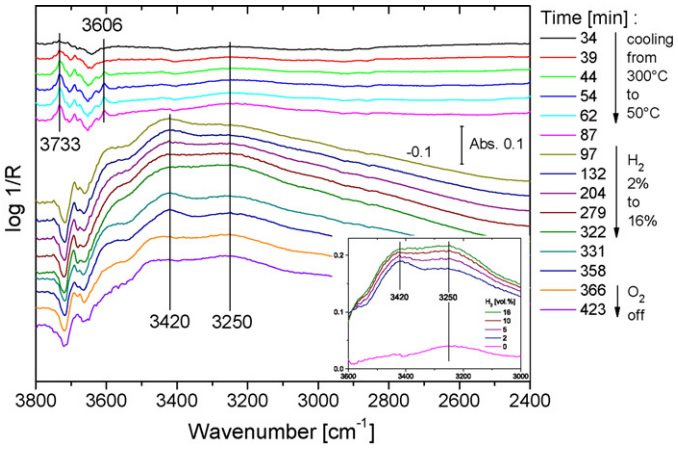

Fig. 6. Hydroxyl region (O–H stretching mode) of the DRIFTS spectra (same spectra as in Figs. 4 and 5). From $t = 97$ min, the spectra have been additionally shifted downwards by 0.1 (in abs. units) with respect to previous spectra, for sake of clarity. Insert: non-shifted DRIFTS spectra (log $1/R$ units) for $t = 87$, 132, 204, 279 and 322 min, allowing to follow the evolution of H_2 pressure-dependent bands.

Fig. 2b shows that the CO_2 rate follows a power law: $r_{CO_2} \propto p_{H_2}^{x}$ where p_{H_2} denotes the hydrogen pressure. The reaction order with respect to hydrogen is: $x = 0.15$. This low value is even lower than that found on Au/Al_2O_3 (0.24) [24]. This will be discussed in Section 3.3.

After switching off H_2, the CO_2 signal decreases significantly and the H_2O signal vanishes gradually. Finally, when the O_2 supply is stopped, the CO_2 signal vanishes as well, as expected.

3.2. Surface species

3.2.1. Carbonyls and carbon dioxide

Regarding the carbonyl region of DRIFTS spectra (Fig. 4), two main features can be distinguished depending on the catalytic conditions: a small peak at 2185–2181 cm^{-1} and a large peak at 2125–2108 cm^{-1}, with a shoulder at ~2135 cm^{-1}. The feature at 2185–2181 cm^{-1} corresponds to CO adsorption on Ti^{4+} (support), while the 2135–2108 cm^{-1} range relates to Au carbonyls (see, e.g., Ref. [33]).

Upon cooling from 300 to 50 °C under $CO + O_2$ mixture, the feature at 2184 cm^{-1} develops, along with a band at 2125–2121 cm^{-1} and its shoulder at ~2135 cm^{-1}. The C–O stretching frequency is directly related to the oxidation state of gold, which in turn is influenced by Au coordination number, Au-support interaction and Au particle size [6,17,34]. Before introduction of H_2, CO is adsorbed on the support and on two kinds of quasi-metallic Au sites, assigned to $Au^{\delta+}$ (~2135 cm^{-1}) and $Au^{\varepsilon+}$ (2125 cm^{-1}), with $0 < \varepsilon < \delta \ll 1$. Based on previous reports [17,34,35], the contribution at ~2135 cm^{-1} may be more precisely ascribed to positively charged low-coordinated gold sites interacting with oxygen at the periphery of essentially metallic gold particles. The coverage of the three species increases when temperature decreases, as can also be seen in Fig. 1b for the main carbonyl peak by looking at intensity versus time. The slight decrease of the peak frequency throughout cooling (2125–2121 cm^{-1}) is due to the increasing coverage of CO on gold [10,16,27,33].

Upon H_2 addition, the intensity of the main carbonyl band ($Au^{\varepsilon+}$–CO) decreases. Fig. 1b shows that it further decreases when H_2 molar fraction increases, and reversibly increases when H_2 is switched off. Fig. 2b allows us to compare the evolution of the CO coverage (θ_{CO}) with that of the CO_2 formation rate (r_{CO_2}). As in the case of CO_2 (see Section 3.1), θ_{CO} follows a power law: $\theta_{CO} \propto p_{H2}^{y}$, where $y = -0.21 \approx -x$ ($x = 0.15$ being the reaction order of CO_2 formation with respect to hydrogen). Thus, r_{CO_2} and θ_{CO} are anti-correlated, most probably due to the lower residence time of CO with increasing conversion rate [27,29].

In the presence of H_2, the Ti^{4+}–CO and $Au^{\delta+}$–CO contributions disappear and the main carbonyl band is shifted from 2121 to 2114 cm^{-1}, i.e. gold is now fully reduced.[2] The disappearance of the feature at ~2135 cm^{-1} may also reflect a change in particle structure and/or in particle-support interaction [34]. After the PrOx experiment, i.e., back to $CO + O_2$ mixture, the peak slightly upshifts to 2116 cm^{-1}, but does not recover its initial position (2121 cm^{-1}) and no shoulder at ~2135 cm^{-1} reappears, i.e., gold sites do not reoxidize.[3]

Hence, as deduced from Figs. 1 and 4, before the PrOx experiment gold is in a slightly cationic form whereas it is Au^0 after it, while the CO_2 formation rate is lower after the PrOx stage as compared to before this stage. This may indicate that partial cationic character of gold reinforces CO oxidation activity, in agreement with some previous reports [6]. More probably, the large amount of water remaining after H_2 switch-off may poison the catalyst [18]. This provides an alternative explanation for the lower CO oxidation rate. In any case, the presence of cationic gold appears not necessary, as demonstrated by the high CO oxidation activity of pure Au^0 in PrOx conditions (Figs. 1 and 2).

Besides, a large band centered at 2349 cm^{-1} (Fig. 3), attributed to CO_2 linearly adsorbed on top of Ti^{4+} [5,16,17,27,36], develops upon cooling the sample in a $CO + O_2$ mixture. Noticeably, this band disappears upon introduction of H_2.

3.2.2. Carbonate-like species (CLS)[4]

Now let us analyze the features observed in the 1700–1200 cm^{-1} region (Fig. 5). Before H_2 supply, under $CO + O_2$ mixture at 300 °C, two broad bands centered at ~1510 and ~1370 cm^{-1} are observed. Upon sample cooling to 50 °C under $CO + O_2$ mixture, the former is replaced by a band at 1576 cm^{-1} while the latter remains present as a broad shoulder of a new and sharper peak at 1437 cm^{-1}, which develops as temperature decreases, together with a sharp peak at 1222 cm^{-1}. Once the temperature has stabilized, those features do not further evolve.

Upon introduction of H_2, the peaks at 1576, 1437 and 1222 cm^{-1} disappear and a large peak at ~1620 cm^{-1}, related to molecularly adsorbed water, appears. This peak does not essentially change while H_2 or O_2 is present in the feed. Three other features at 1668, 1558 and 1248 cm^{-1} emerge upon H_2 introduction, but those vanish simultaneously when the H_2 molar fraction is increased. In addition, a small contribution at 1396 cm^{-1} comes out within the broad band centered at ~1370 cm^{-1}, which is still present. The two peaks at 1668 and 1248 cm^{-1} reappear upon H_2 switch-off, together with one at ~1440 cm^{-1}. Only a slight modification of the 1450–1350 cm^{-1} region can be noticed during CO oxidation. Finally, all the previous peaks vanish when the flow of O_2 is also set to zero, and a broad band at ~1570 cm^{-1} (re)appears.

Haruta et al. have observed features (similar to ours) at 1592, 1430 and 1221 cm^{-1} by adsorbing CO on Au/TiO_2, and have ascribed them to noncoordinated (1592 and 1430 cm^{-1}) and bidentate (1221 cm^{-1}) carbonate species [25]. Boccuzzi et al. have observed most of our features for Au/TiO_2 exposed to $CO + O_2$ mixture, and have attributed them to bicarbonate (1582, 1413 and 1220 cm^{-1}) and carboxylate (1670 and 1243 cm^{-1}) species [29]. Tanaka and White have adsorbed CO_2 on anatase predosed with water and have measured infrared bands at 1671, 1420 and 1245 cm^{-1}, which have been assigned to bidentate carbonate (1671 and 1245 cm^{-1}) and bicarbonate (1420 cm^{-1}) species [37]. Our peak at 1248 cm^{-1} may alternatively correspond to a hydroxycarbonyl intermediate, according to Kung et al. [5]. In addition, the feature at 1440 cm^{-1} has been previously assigned to a monodentate carbonate [10], and that at 1576 cm^{-1} to a bidentate carbonate [38] or carboxylate [16].

From these partly contradictory assignments published in the literature, it appears difficult to identify all the observed species without further studies (e.g., by using O and C isotopes). Nevertheless, we can assert that some CLS (~1510 cm^{-1}, which is the major contribution over the entire experiment, and ~1370 cm^{-1} see Fig. 3) have already formed during CO oxidation on Au/TiO_2 at 300 °C. As the sample is cooled down to 50 °C,

[2] According to Schumacher et al., this shift may result from charge donation from the partly reduced substrate or, preferably, from indirect interaction of H and O species coadsorbed on the Au nanoparticles [10]. However, in their case, the C–O frequency is downshifted by only 3 cm^{-1} in the presence of H_2.

[3] After O_2 switch-off, this peak downshifts to 2108 cm^{-1}. Comparable shifts have been measured by others in similar experiments [10,22]. The partial reduction of TiO_2 by CO, leading to negative charging of the Au particles, could explain this shift [4,22,29].

[4] Compact formulas of some carbon-containing species potentially adsorbed on the catalyst. Carbonate: CO_3; bicarbonate (i.e., hydrogenocarbonate): CO_2OH; carboxylate: CO_2; hydroxycarbonyl (i.e., carboxylic acid): COOH. Formate: HCO_2.

simultaneously to the appearance of adsorbed CO_2, other CLS form (1576, 1437 and 1222 cm^{-1}, assigned to bicarbonates), but in small amounts, as shown by the moderate band intensities (Fig. 5). Essentially no additional CLS are formed under CO + O_2 at steady state.[5]

In addition to particle sintering and change in the Au oxidation state, build up of a carbonate layer on the support is often mentioned as a possible cause of on-stream deactivation during low-temperature CO oxidation [5,9,10,13,15–20,26,27]. These CLS would be in dynamic equilibrium with adsorbed and gaseous CO_2 [28] and would block adsorption sites on the support or at the particle/support interface, where oxygen activation may take place. The extent of activity decline, which is not significant here, depends on several parameters such as nature of the support, preparation method, type of pre-treatment and experimental conditions. CLS have also been considered as spectator by-products [16,27,28]. In our case, it is probable that the broad feature at ~1370 cm^{-1} is a spectator carbonate [10], since it is present all along the experiment (Fig. 5). The nature and the role of CLS will be further discussed in Section 3.3.

3.2.3. Water and hydroxyls

Fig. 6 shows sharp peaks for wavenumbers higher than ~3600 cm^{-1} (3733 and 3606 cm^{-1}), observed before introduction of H_2. They correspond to isolated hydroxyl groups on TiO_2 (see, e.g., Ref. [10]). These peaks grow with time while cooling the sample, due to the presence of water (~100 vol. ppm) in the feed.[6] In addition, a broad band can be seen around ~3250 cm^{-1} (see also the insert of Fig. 6). Upon addition of H_2 to the CO + O_2 feed, features above 3600 cm^{-1} decrease and a large band quickly develops in the ~3500–3200 cm^{-1} region, which relates to the ν(O–H) vibration mode in hydrogen-bonded hydroxyl groups and water adsorbed at the catalyst surface.

As mentioned above, the introduction of H_2 also induces the appearance of an intense band at ~1620 cm^{-1}, which corresponds to the δ(HOH) vibration mode of adsorbed water. Whereas the ν(O–H) band grows with H_2 content (mainly around ~3250 cm^{-1}, see insert of Fig. 6), the δ(HOH) band is stable (Fig. 5). As a consequence, under PrOx conditions, both water and OH groups are present on the surface. We propose that the band at ~3250 cm^{-1} relates, at least in part, to OH (or OOH) species loosely bonded on the Au particles and/or at their periphery. As a matter of fact, we have recently detected a DRIFTS band centered at the same frequency on unsupported gold under PrOx conditions [23]. Moreover, Boccuzzi et al. have assigned a band centered at 3320 cm^{-1} to Au–OH species formed during water-gas shift on Au/TiO_2 [29]. In summary, TiO_2 would be (at least partly) covered with OH and water as soon as H_2 is introduced in the feed, and increasing further the H_2 content would increase the concentration of Au-bonded hydroxyls. The existence of these species has already been hypothesized following various experimental observations [13,39–42] and the stability of Au–OH species has been checked in several theoretical works [40,43,44].

The ν(O–H) features decline slowly when H_2 (then O_2) supply is stopped, in parallel to the slow evacuation of water from the reactor (Fig. 1a), as we observed for unsupported Au under similar conditions [23].

[5] Unlike Schumacher et al. [10], we observed no formates on the catalyst. Actually, these authors might have encountered contamination by hydrocarbons, as suggested by the vibration they observed at 2972 cm^{-1} and could not attribute. This would also explain the high deactivation rate of their Au/TiO_2 catalyst, together with the decrease of the CO coverage with time, even in the presence of H_2.

[6] The presence of water could explain the absence of deactivation in H_2-free atmosphere (Fig. 1a).

3.3. PrOx mechanism

At 50 °C under H_2-free conditions, the catalyst surface is covered with CO, CO_2 and carbonate-like species. In the presence of H_2, CO_2 and CLS are essentially replaced by H_2O and OH groups. H_2 has a dramatic effect on the CO oxidation rate: from 0 to 16 mol.% of H_2, the PrOx activity exhibits a twofold increase, while the selectivity decreases by only ~20% (Fig. 2). Previous studies of CO oxidation on Au/TiO_2 have not shown any boosting effect of co-fed H_2, but only regeneration [10,15]. It is possible that the very high amounts of H_2 used in these studies (for example, Schumacher et al. used a H_2/CO molar ratio of 75 [10], while ratios ranging from 1 to 8 were used in the present work) induced poisoning of the catalyst surface by water. The surface-science batch conditions we employed in a previous study may have caused the same effect [15]. Shou et al. have evidenced a comparable promotional effect of H_2 on an Au/TiO_2 catalyst loaded with FeOx [21]. Following the mechanism proposed by Daniells et al. [20], they have suggested that the interaction of water with CO adsorbed at Au–Fe sites allows the formation of a hydroxycarbonyl intermediate, which decomposes to CO_2 and H_2O. Here we have demonstrated that the presence of Fe is not necessary to observe boosting by H_2.

Actually, the mechanism of Daniells et al. is based on the model initially proposed by Bond and Thompson [3] and later refined by Kung and co-workers [5,13]. The latter involves the insertion of an Au-bonded CO molecule into an Au^+–OH bond to form a hydroxycarbonyl. This species is oxidized to a bicarbonate, which decomposes into Au^+–OH and CO_2. By reacting with poisoning carbonates, water would produce a hydroxyl and an active bicarbonate, and thus regenerate the catalyst. Similarly, the reaction of H_2 with a carbonate would produce a hydroxyl and a formate, which in turn would react with O_2 to form a bicarbonate [5]. However, this mechanism has been derived from CO oxidation experiments involving Au/Al_2O_3 catalysts with high initial activity and high deactivation rate. In our case of PrOx over Au/TiO_2, neither Au^+ nor formate or bicarbonate species are detected on the sample (Figs. 4 and 5).

Another alternative to the CO^{ad} + O^{ad} simplest model has been proposed by Daté et al. [19], on the basis of experiments showing water-induced promotion of CO oxidation on several catalysts, including Au/TiO_2. In this mechanism, $O_2{}^{ad}$ would react with H_2O^{ad} at the gold particle periphery to form two hydroxyl groups and active oxygen, which is able to react with CO^{ad} to form CO_2 via a carboxylate. Deactivation occurs through the formation of a carbonate. Reaction of this species with water yields a bicarbonate, which readily decomposes to CO_2 and OH^{ad}, just like in the mechanism proposed by Kung and co-workers. Here, the promotional role of water is double: activation of oxygen and decomposition of carbonates. This model could be compatible with our data, taking into account that water is formed by reaction between H_2 and O_2. In particular, the species we detect at low H_2 pressure (1668 + 1248 cm^{-1}, plus 1558 cm^{-1} upon H_2 introduction or ~1440 cm^{-1} upon H_2 evacuation, Fig. 5) is most probably a carboxylate (Section 3.2.2).

However, it has been shown that CO oxidation can be favoured without production of water during PrOx at near-room temperature [23,24]. In our case, the strong decrease of the CO oxidation rate upon H_2 (fast) switch-off, in spite of the large residual amount of (slowly declining) water (Fig. 1a), suggests that H_2O^{ad} is not a key-intermediate. In order to explain the hydrogen-induced promotion of CO oxidation on Au/Al_2O_3 and unsupported Au, a new pathway has been proposed on the basis of kinetic, calorimetric and theoretical studies of water formation from H_2 and O_2 on silica-supported gold, by Barton and Podkolzin [40]. According to these authors, the reaction rate would be determined

by the following step:

$$OOH^{ad} + H_2 \rightarrow H_2O_2{}^{ad} + H^{ad} \quad (S1)$$

Generation of hydroperoxy intermediates from synergy between H_2 and O_2 would be driven by the formation of O–H bonds that enhance O–Au interactions [45]. Actually, these highly oxidative intermediates have been identified by inelastic neutron scattering at the surface of a Au/TiO_2 catalyst exposed to $H_2 + O_2$ [46] and by combined UV–vis/X-ray absorption spectroscopy during propylene epoxidation with O_2 and H_2 on Au–Ba/Ti–SiO_2 [47]. Moreover, several other studies on the promotional effect of water have shown the ability of water-related species to oxidize CO [39,41,42,44]. In the absence of CO or propylene, these species would be readily converted to water via OH intermediates [40]. We propose that during PrOx, the formation of CO_2 may result from the reaction of CO with one of these species, e.g.:

$$CO^{ad} + OOH^{ad} \rightarrow HCO_3{}^{ad} \rightarrow CO_2{}^{ad} + OH^{ad} \rightarrow CO_2 + OH^{ad} \quad (S2)$$

This series of steps involves hydroxyl groups, which we do observe, possibly adsorbed on Au (Fig. 6). It could proceed via a bicarbonate intermediate, as in the Kung's and Daté's models. Moreover, the above pathway is compatible with a positive reaction order towards H_2 (Fig. 2b). The very low value of the CO oxidation order (0.15) is consistent with a chain-like mechanism, in which a low concentration of H_2 is necessary and sufficient to produce OOH radicals [24], the amount of H atoms being unaltered by the overall (S2) reaction.

As for the previous model accounting for promotion by water [19], this additional "hydroperoxy pathway", although hypothetical, is consistent with our data and offers a rational explanation of the promotion of CO oxidation by hydrogen on Au-based catalysts. In fact, to reconcile water and hydrogen-promoting mechanisms, it is possible that adsorbed water forms active hydroperoxy intermediates, but with higher activation energy than co-adsorbed H_2 and O_2 do. This way, both promotional effects would be of similar nature. Future experiments will aim at clarifying this point.

4. Conclusions

The effect of H_2 addition on the kinetics and mechanism of CO oxidation over a reference Au/TiO_2 catalyst has been investigated by DRIFTS–MS. The reaction was mainly performed at 50 °C, under $CO + O_2$ (2 mol.% of each gas) in a He flow. The H_2 content was varied between 2 and 16 mol.%. Our main conclusions are summarized below.

- Addition of H_2 to the $CO + O_2$ feed increases CO oxidation rate by up to a factor of ~2, without extensive loss of selectivity towards CO_2 (>80%). The CO oxidation order with respect to H_2 is 0.15.
- While CO is adsorbed on Ti^{4+} and $Au^{\delta+}$ sites before introduction of H_2, only $CO–Au^0$ species are detected in the presence (and after evacuation) of H_2. Hence the presence of cationic gold is not a requisite for CO oxidation in such conditions.
- Carbonate-like species (carbonates and bicarbonates, no formates) and CO_2 are adsorbed on the catalyst in H_2-free atmosphere. Under PrOx conditions, the surface is almost free of carbonate-like species, except under low H_2 pressure, where sharp infrared features assignable to carboxylates were recorded.
- Addition of H_2 to the $CO + O_2$ feed induces the formation of adsorbed H_2O and OH groups. Au–OH species are suggested to develop when the H_2 pressure increases.

From these results and the analysis of recent spectroscopic experiments, we propose that PrOx may proceed via the reaction of Au-bonded CO with hydroperoxy (OOH) intermediates that would originate from H_2 and O_2 co-adsorption on metallic gold. This mechanism does not exclude the possibility that bicarbonates and carboxylates were also involved in the CO_2 formation pathway.

Acknowledgements

LP thanks Dr Stéphane Loridant and Dr Valérie Caps for fruitful discussions. LP and AV are grateful to Robbie Burch's group for receiving them at CenTACat laboratory through the EU-funded Transnational Access Program.

References

[1] D.T. Thompson, Nano Today 2 (2007) 40 (And References therein).
[2] M. Haruta, T. Kobayashi, H. Sano, N. Yamada, Chem. Lett. 4 (1987) 405.
[3] G.C. Bond, D.T. Thompson, Gold Bull. 33 (2000) 41 (And References therein).
[4] M. Chen, D.W. Goodman, Acc. Chem. Res. 39 (2006) 739 (And references therein).
[5] M.C. Kung, R.J. Davis, H.H. Kung, J. Phys. Chem. C 111 (2007) 11767 (And references therein).
[6] J.C. Fierro-Gonzales, B.C. Gates, Catal. Today 122 (2007) 201 (And references therein).
[7] R.M. Torres Sanchez, A. Ueda, K. Tanaka, M. Haruta, J. Catal. 168 (1997) 125.
[8] R.J.H. Grisel, B.E. Nieuwenhuys, J. Catal. 199 (2001) 48.
[9] M.M. Schubert, V. Plzak, J. Garche, R.J. Behm, Catal. Lett. 76 (2001) 143.
[10] B. Schumacher, Y. Denkwitz, V. Plzak, M. Kinne, R.J. Behm, J. Catal. 224 (2004) 449.
[11] C. Rossignol, S. Arrii, F. Morfin, L. Piccolo, V. Caps, J.L. Rousset, J. Catal. 230 (2005) 476.
[12] J.T. Calla, R.J. Davis, Ind. Eng. Chem. Res. 44 (2005) 5403.
[13] C.K. Costello, M.C. Kung, H.S. Oh, Y. Wang, H.H. Kung, Appl. Catal. A 232 (2002) 159.
[14] M. Manzoli, A. Chiorino, F. Boccuzzi, Appl. Catal. B 52 (2004) 259.
[15] M. Azar, V. Caps, F. Morfin, J.L. Rousset, A. Piednoir, J.C. Bertolini, L. Piccolo, J. Catal. 239 (2006) 307.
[16] M.A. Bollinger, M.A. Vannice, Appl. Catal. B 8 (1996) 417.
[17] F. Boccuzzi, A. Chiorino, M. Manzoli, P. Lu, T. Akita, S. Ichikawa, M. Haruta, J. Catal. 202 (2001) 256.
[18] M. Daté, M. Haruta, J. Catal. 201 (2001) 221.
[19] M. Daté, M. Okumora, S. Tsubota, M. Haruta, Angew. Chem., Int. Ed. 43 (2004) 2129.
[20] S.T. Daniells, M. Makkee, J.A. Moulijn, Catal. Lett. 100 (2005) 39.
[21] M. Shou, H. Takekawa, D.Y. Ju, T. Hagiwara, D.L. Lu, K.I. Tanaka, Catal. Lett. 108 (2006) 119.
[22] M. Daté, H. Imai, S. Tsubota, M. Haruta, Catal Today 122 (2007) 222.
[23] E. Quinet, L. Piccolo, H. Daly, F.C. Meunier, F. Morfin, A. Valcarcel, F. Diehl, P. Avenier, V. Caps, J.L. Rousset, Catal. Today 138 (2008) 43.
[24] E. Quinet, F. Morfin, F. Diehl, P. Avenier, V. Caps, J.L. Rousset, Appl. Catal. B 80 (2008) 195.
[25] M. Haruta, S. Tsubota, T. Kobayashi, H. Kageyama, M.J. Genet, B. Delmon, J. Catal. 144 (1993) 175.
[26] P. Konova, A. Naydenov, C. Venkov, D. Mehandjiev, D. Andreeva, T. Tabakova, J. Mol. Catal. A 213 (2004) 235.
[27] B.K. Chang, B.W. Jang, S. Dai, S.H. Overbury, J. Catal. 236 (2005) 392.
[28] J.C. Clark, S. Dai, S.H. Overbury, Catal. Today 126 (2007) 135.
[29] F. Boccuzzi, A. Chiorino, M. Manzoli, D. Andreeva, T. Tabakova, J. Catal. 188 (1999) 176.
[30] F.C. Meunier, A. Goguet, S. Shekhtman, D. Rooney, H. Daly, Appl. Catal. A 340 (2008) 196.
[31] F.C. Meunier, D. Reid, A. Goguet, S. Shekhtman, C. Hardacre, R. Burch, W. Deng, M. Flytzani-Stephanopoulos, J. Catal. 247 (2007) 277.
[32] J. Sirita, S. Phanichphant, F.C. Meunier, Anal. Chem. 79 (2007) 3912.
[33] S. Derrouiche, P. Gravejat, D. Bianchi, J. Am. Chem. Soc. 126 (2004) 13010.
[34] T. Venkov, K. Fajerwerg, L. Delannoy, H. Klimev, K. Haadjivanov, C. Louis, Appl. Catal. A 301 (2006) 106.
[35] S. Minico, S. Scire, C. Crisafulli, A.M. Visco, S. Galvagno, Catal. Lett. 47 (1997) 273.
[36] G. Martra, Appl. Catal. A 200 (2000) 275.
[37] K. Tanaka, J.M. White, J. Phys. Chem. 86 (1982) 4708.
[38] L.F. Liao, C.F. Lien, D.L. Shieh, M.T. Chen, J.L. Lin, J. Phys. Chem. B 106 (2002) 11240.
[39] M.A. Sanchez-Castillo, C. Couto, W.B. Kim, J.A. Dumesic, Angew. Chem., Int. Ed. 43 (2004) 1140.
[40] D.G. Barton, S.G. Podkolzin, J. Phys. Chem. B 109 (2005) 2262–2274.
[41] T.S. Kim, J. Gong, R.A. Ojifinni, J.M. White, C.B. Mullins, J. Am. Chem. Soc. 128 (2006) 6282.
[42] W.C. Ketchie, M. Murayama, R.J. Davis, Top. Catal. 44 (2007) 307.
[43] M. Suh, P.S. Bagus, S. Pak, M.P. Rosynek, J.H. Lunsford, J. Phys. Chem. B 104 (2000) 2736.
[44] A. Bongiorno, U. Landman, Phys. Rev. Lett. 95 (2005) 106102.
[45] L. Barrio, P. Liu, A. Rodriguez, J.M. Campos-Martin, J.L.G. Fierro, J. Phys. Chem. C 111 (2007) 19001.
[46] C. Sivadinarayana, T.V. Choudhary, L.L. Daemen, J. Eckert, D.W. Goodman, J. Am. Chem. Soc. 126 (2004) 38.
[47] J.J. Bravo-Suarez, K.K. Bando, J. Lu, M. Haruta, T. Fujitani, S.T. Oyama, J. Phys. Chem. C 112 (2008) 1115.